Available online at www.sciencedirect.com
SCIENCE DIRECT®
PERGAMON
International Journal of Heat and Mass Transfer 46 (2003) 3511–3520
International Journal of HEAT and MASS TRANSFER
www.elsevier.com/locate/ijhmt

Laser shortpulse heating of gold: variable properties case

Bekir Sami Yilbas *

Department of Mechanical Engineering, King Fahd University of Petroleum and Minerals, Dhahran 31261, Saudi Arabia

Received 6 November 2001; received in revised form 2 January 2003

Abstract

Laser shortpulse heating of metallic substrates requires microscopic examination of the energy transport in the irradiated region. This is because of low specific heat capacity of electrons, which results in nonequilibrium temperature distribution in this region. In the present study, laser shortpulse heating of gold with variable properties is considered. Nonequilibrium energy transport is modelled using an electron kinetic theory approach. The resulting integro-differential equations are reduced to partial differential equation using a Fourier transform method. The resulting differential equation is further transformed into two differential equations similar to those given in the two-equation model. The coefficients of the differential equations are correlated. It is found that variable properties results in higher lattice site and lower electron temperatures as compared to those corresponding to constant properties case.

1. Introduction

When a laser short pulse interacts with a solid substrate, nonequilibrium energy exchange occurs in the region irradiated by a laser beam. Electrons absorb energy from the irradiated field and transfer their excess energy to lattice site through collisional process. Since the specific heat capacity of electrons is lower than the lattice site specific heat capacity and electrons only transfer some fraction of their excess energy to lattice site during a short period of interaction, electron temperature well excess of lattice temperature is resulted. Consequently, energy transfer mechanism during short duration of interaction cannot be described by a classical Fourier heating model; therefore, microscopic level of examination of the problem is necessary.

Considerable research studies were carried out to model the laser shortpulse heating process. Anisimov et al. [1] addressed nonequilibrium energy transport for laser short pulse heating process. The nonlocal heat transport due to steep temperature gradients was examined by Luciani et al. [2]. They indicated that a nonlocal macroscopic formula developed, as comparable to Fokker–Planck equation, represented successfully the heat transport due to steep temperature gradient. Nonequilibrium heating due to femtosecond pulse heating of tungsten was investigated by Fujimoto et al. [3]. They showed that electron temperature well excess of phonon temperature occurred and electron–phonon energy relaxation time of several hundred femtoseconds was resulted. Nonequilibrium electron and lattice temperatures were studied by Elsayed-Ali et al. [4]. Electron–phonon energy transfer was time resolved and it was observed that electron–phonon energy transfer occurred within in 1–4 ps, which increased with increasing laser energy. An experimental investigation for electron–phonon coupling in metallic superconductors was carried out by Brorson et al. [5]. They indicated that the measurement results agreed well with the theoretical predictions obtained by Allen [6]. The hyperbolic heat conduction due to a mode locked laser pulse train was studied by Hector et al. [7]. They showed that the hyperbolic temperature profile in a finite region exceeded that in a semi-infinite medium, since waves reflected from the insulated boundary overlapped the waves travelling towards the insulated boundary. The nonlinear hyperbolic and parabolic heat conduction due to shortpulse heating were studied for various boundary conditions by Kar et al. [8]. They indicated that the effects of temperature dependent thermal properties had a

* Tel.: +966-3-860-2540; fax: +966-3-860-2949.
E-mail address: bsyilbas@kfupm.edu.sa (B.S. Yilbas).

0017-9310/03/$ - see front matter © 2003 Elsevier Science Ltd. All rights reserved.
doi:10.1016/S0017-9310(03)00131-5

Nomenclature

A	$A = \frac{fk\tau_s}{\lambda^2}$
B	$(B = k)$ where k is thermal conductivity (W/m K)
C	$C = \frac{fk}{\lambda^2}\left(1 - \frac{k\tau_s}{\rho Cp\lambda^2}\right)$
D	$D = \rho Cp - \frac{fk\tau_s}{\lambda^2}$
ABS	Absolute value
C_e	electron heat capacity (J/m^3 K)
C_l	lattice heat capacity (J/m^3 K)
Cp	specific heat of lattice site (J/kg K)
ΔE	energy transferred to lattice site (J)
f	fraction of excess energy exchange
G	electron–phonon coupling factor (W/m^3 K)
I_o	laser peak power intensity (W/m^2)
k	thermal conductivity (W/m K)
k_B	Boltzmann's constant (1.38×10^{-23} J/K)
m_e	electron mass (kg)
N	electron number density (1/m^3)
r_f	reflection coefficient
S	source term
T_l	lattice site temperature (K)
T_e	electron temperature (K)
T_d	Debye temperature (K)
t	Time (s)
Δt	rime increment (s)
$\overline{V}$	electron mean velocity (m/s)
s	spatial coordinates corresponding to the electron movement (m)
x	spatial coordinates corresponding to the x-axis for phonon (m)
Δx	spatial increment (m)
α	thermal diffusivity (m^2/s)
δ	absorption coefficient (1/m)
λ	mean free path of electrons (m)
ρ	density (kg/m^3)
τ_p	electron mean free time between electron–phonon coupling (s)
τ_s	electron–phonon characteristic time ($\tau_s = G/C_e$) (s)

significant effect on the resulting temperature field. A relaxation model for heat conduction and generation was introduced by Malinowski [9]. He observed that unlike the classical hyperbolic model, the relaxation solutions generally did not tend to approach the corresponding parabolic solutions. Heating of opaque surfaces by picosecond laser pulses was studied by Strehlow [10]. He demonstrated that the existence of a lower threshold for measurable evaporation and ablation of the surface increased drastically once the temperature reached to initial temperature at the surface. Size effects on nonequilibrium laser heating of metal films were investigated by Qiu and Tien [11]. They showed that the size effect reduced the effective thermal conductivity and increased the electron–phonon energy exchange rate. A unified filed approach for heat conduction from macro-to-micro scales was investigated by Tzou [12]. He showed that the microscale interaction between phonons and electrons and the inert behavior of molecules at low temperatures are two physical factors in the macroscopic lagging response in the model proposed. Cheng [13] presented heat-conduction equations, which were derived from the Boltzmann equations. He indicated that the equations derived were a better approximation than the Fourier law and Cattaneo equation for heat conduction at the scales when the characteristic length (film thickness) was comparable to the heat-carrier mean free path and/or characteristic time (laser pulse width).

An electron kinetic theory approach was introduced by Yilbas [14] to accommodate nonequilibrium energy transfer during laser heating process. He demonstrated that the predictions of the electron kinetic theory approach became similar to the results obtained from the Fourier heating model once the duration of the heating pulse exceeded nanoseconds [15]. Electron kinetic theory approach was extended to include three-dimensional effects on the heating process [16]. However, the thermal properties of the substrate material were kept constant (independent of temperature) in the simulations. In the present study, electron kinetic theory is considered to model the laser short pulse heating of gold. The thermal properties of gold are considered as temperature dependent. The integro-differential equations governing the nonequilibrium energy transport are reduced to two differential equations as similar to those presented in the two-equation model [17]. The coefficients of resulting differential equations are correlated with the coefficients of those equations presented in the two-equation model.

2. Mathematical analysis of heating process

The mathematical arrangements of two-equation model and electron kinetic theory approach are presented briefly, since the details of the analyses can be found elsewhere [13,17,18].

2.1. Two-equation model

The two-equation model representing the energy exchange mechanism during phonon absorption and

electron–phonon coupling after one-dimensional consideration can be written as [17]:

$$C_e\frac{\partial T_e(s,t)}{\partial t}=\nabla\cdot(k\nabla T_e(s,t))-G[T_e(s,t)-T_l(x,t)]+S$$
$$C_l\frac{\partial T_l(x,t)}{\partial t}=G[T_e(s,t)-T_l(x,t)] \quad (1)$$

$T_e(s,t)$ and $T_l(x,t)$ are the electron and lattice site temperatures, S is the laser source term ($I_o\delta\exp(-\delta x)$), and C_e and C_l are the electron and lattice heat capacities, respectively. G is the electron–phonon coupling factor, given by:

$$G=\frac{\pi^2 m_e N\overline{V}^2}{6\tau_p T_e(s,t)} \quad (2)$$

where m_e, N, $\overline{V}$, and τ_p are electron mass, electron number density, electron drift velocity and the electron mean free time between electron–phonon coupling respectively.

2.2. Electron kinetic theory approach

The energy transport in the region irradiated by a laser shortpulse occurs due to electron–phonon coupling process in the electron–phonon sub-systems. In the electron kinetic theory approach, the energy transport is modelled using a probabilistic approach and energy method. The mathematical model pertinent to electron kinetic approach is given in the previous study [14,19], hence, the resulting integro-differential equations are given.

The complete equation for the electron—lattice site atom collision process is:

$$\frac{\partial}{\partial t}\left[(\rho CpT_l(x,t))+\tau_s\frac{\partial}{\partial t}(\rho CpT_l(x,t))\right]=\int_{-\infty}^{\infty}\frac{N_{sx}\overline{V}fk_B}{\lambda^2}\exp\left(-\frac{|x-s|}{\lambda}\right)T_e(s,t)\,ds-\int_{-\infty}^{\infty}\frac{N_{sx}\overline{V}fk_B}{\lambda^2}\exp\left(-\frac{|x-s|}{\lambda}\right)T_l(x,t)\,ds+\int_{-\infty}^{\infty}\frac{I_o f}{\lambda^2}\frac{N_{sx}}{N_{sx}+N_{xs}}\times\exp\left(-\frac{|x-s|}{\lambda}\right)\int_x^s f'(x)\,d\xi\,ds \quad (3)$$

where f is the fraction of electron excess energy, which transfers to lattice site during a single electron lattice site collision, and τ_s is electron–phonon characteristic time. The analysis related to f is given in Appendix A. The first term on the left hand side of Eq. (3) is energy gain by the substrate material through collisional process, first and second terms on the right hand side represent electron and lattice energies, and third term on the right hand site is the energy gain of the electrons due to the irradiated field. The final temperature of the electrons in dx after the collision process can be readily found from the conservation of energy, i.e.:

Total electron energy after collision = Total electron energy in during dt *− Change of lattice site energy*

Total electron energy after collision:

$$\int_{-\infty}^{\infty}\frac{N_{sx}\overline{V}(1-f)k_B}{\lambda^2}\exp\left(-\frac{|x-s|}{\lambda}\right)T_e(s,t)\,ds \quad (4)$$

Total electron energy carried into dx during dt is:

$$\int_{-\infty}^{\infty}\frac{N_{sx}\overline{V}k_B}{\lambda^2}\exp\left(-\frac{|x-s|}{\lambda}\right)T_e(s,t)\,ds+\int_{-\infty}^{\infty}\frac{I_o f}{\lambda^2}\times\frac{N_{sx}}{N_{sx}+N_{xs}}\exp\left(-\frac{|x-s|}{\lambda}\right)\int_x^s f'(\xi)\,d\xi\,ds \quad (5)$$

and the change of lattice site atom energy is:

$$\frac{\partial}{\partial t}\left[\rho CpT_l(x,t)+\tau_s\rho Cp\frac{\partial}{\partial t}(T_l(x,t))\right] \quad (6)$$

Consequently, substituting the Eqs. (3)–(5) into the requirement of the conservation of energy gives:

$$\int_{-\infty}^{\infty}\frac{N_{sx}\overline{V}k_B}{\lambda^2}\exp\left(-\frac{|x-s|}{\lambda}\right)[T_e(s,t)-fT_l(x,t)]\,ds=\int_{-\infty}^{\infty}\frac{N_{sx}\overline{V}k_B}{\lambda^2}\exp\left(-\frac{|x-s|}{\lambda}\right)(1-f)\theta(s,t)\,ds+\int_{-\infty}^{\infty}(1-f)\frac{N_{sx}}{N_{sx}+N_{xs}}\times\exp\left(-\frac{|x-s|}{\lambda}\right)\int_x^s f'(\xi)\,d\xi\,ds \quad (7)$$

It should be noted that electron energy, which is characterized by temperature $T_e(s,t)$, is augmented from the initial $T_e(s,t)$ by an amount equal to that absorbed in travelling from s to x (Fig. 1). The total amount of energy, which is absorbed in an element $d\xi$, area A in time dt is:

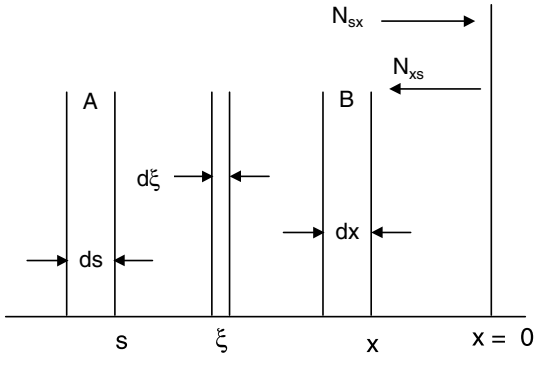

Fig. 1. Electron movement in the surface region ($x=0$ is the free surface).

$$I_o A\,\mathrm{d}t\,\mathrm{d}\xi f'(\xi) \tag{8}$$

where I_o is the laser power intensity, since all the beam energy is absorbed in the x-axis. The electron density can vary along the x-axis, in particular, the number of electrons travelling from ds to dx may not be the same as that from dx to ds. Therefore, the portion of energy which is absorbed by electrons which travel from ds to dx in dt is:

$$I_o A\,\mathrm{d}t f'(\xi)\,\mathrm{d}\xi \frac{N_{sx}}{N_{sx}+N_{xs}} \tag{9}$$

where N_{sx} and N_{xs} are the number of electrons which travel from s to x and from x to s, respectively (Fig. 1). The total number of electrons which travel from ds to dx in this time is:

$$N_{sx} A\overline{V}\,\mathrm{d}t \tag{10}$$

where $\overline{V}$ is electron mean velocity. Hence, the average energy absorbed by one electron in dξ in time dt is:

$$I_o \frac{f'(\xi)\,\mathrm{d}\xi}{(N_{sx}+N_{xs})\overline{V}} \tag{11}$$

and the total amount of energy absorbed by this electron from dx to ds is:

$$\int_x^s \frac{f'(\xi)\,\mathrm{d}\xi}{(N_{sx}+N_{xs})\overline{V}} \tag{12}$$

Eq. (12) gives the extra energy gain by the electrons which travel from ds to dx.

Eqs. (3) and (7) have been kept in general; however, it may be useful to consider a particular case, where electrons cannot escape through the surface (which may equally apply when a steady state space charge exists).

In this case, the assumption that all directions of travel are equally probable results in:

$$\begin{aligned}\frac{\partial}{\partial t}\left[\rho CpT_l(x,t)+\tau_s\frac{\partial}{\partial t}(\rho CpT_l(x,t))\right] &= \int_{-\infty}^{\infty}\frac{fk}{\lambda^3}\exp\left(-\frac{|x-s|}{\lambda}\right)T_e(s,t)\,\mathrm{d}s \\ &\quad -\int_{-\infty}^{\infty}\frac{fk}{\lambda^3}\exp\left(-\frac{|x-s|}{\lambda}\right)T_l(x,t)\,\mathrm{d}s \\ &\quad +\int_{-\infty}^{\infty}\frac{I_o f}{\lambda^2}\exp\left(-\frac{|x-s|}{\lambda}\right)\int_x^s f'(x)\,\mathrm{d}\xi\,\mathrm{d}s\end{aligned} \tag{13}$$

which makes use of the simple kinetic theory result for the electron thermal conductivity [20]:

$$k=\frac{N\overline{V}k_B\lambda}{3} \tag{14}$$

and

$$\begin{aligned}&\left[\int_{-\infty}^{\infty}\frac{k}{\lambda^3}\exp\left(-\frac{|x-s|}{\lambda}\right)[T_e(s,t)-fT_l(x,t)]\,\mathrm{d}s\right] \\ &\quad=\int_{-\infty}^{\infty}\frac{k}{\lambda^3}\exp\left(-\frac{|x-s|}{\lambda}\right)(1-f)T_e(s,t)\,\mathrm{d}s \\ &\qquad+\int_{-\infty}^{\infty}(1-f)\exp\left(-\frac{|x-s|}{\lambda}\right)\int_x^s f'(x)\,\mathrm{d}\xi\,\mathrm{d}s\end{aligned} \tag{15}$$

Eqs. (13) and (15) are the energy transport equations of interest for laser short pulse heating process. The method of solution to be used in the following analysis is the transformation of the simultaneous differential—integral Eqs. (13) and (15) using the Fourier integral transformation, with respect to x [21]. This is due to the fact that the resultant ordinary differential equations may then be handled much more conveniently. Consider first reduction of the set of equations to the differential equation of heat conduction.

The Fourier transformation of a function $f(x)$ is defined by:

$$F[f(x)]=\int_{-\infty}^{\infty}\exp(-\mathrm{i}\omega x)f(x)\,\mathrm{d}x=F(\omega) \tag{16}$$

and the Fourier inversion by:

$$f(x)=\frac{1}{2\pi}\int_{-\infty}^{\infty}F(\omega)\exp(-\mathrm{i}\omega x)\,\mathrm{d}\omega \tag{17}$$

The Fourier transformation of the convolution integral:

$$\int_{-\infty}^{\infty}f(\xi)g(x-s)\,\mathrm{d}s \tag{18}$$

is the produces of the transforms:

$$\bar{f}(\omega)\cdot\bar{g}(\omega) \tag{19}$$

and the transform of function $\exp\left(-\frac{|x|}{\lambda}\right)$ is

$$\frac{2\lambda}{1+\omega^2\lambda^2} \tag{20}$$

Therefore, the Fourier transform of the function:

$$IX=\int_{-\infty}^{\infty}\frac{k}{\lambda^3}\exp\left(-\frac{|x-s|}{\lambda}\right)T_l(x,t)\,\mathrm{d}s \tag{21}$$

will be a constant factor (the value of integral) multiplying the transform of the function $T_l(x,t)$, i.e.:

$$F[IX]=\frac{kf}{\lambda^3}\overline{T}_l F\left\{\int_{-\infty}^{\infty}\exp\left(-\frac{|x-s|}{\lambda}\right)\mathrm{d}s\right\} \tag{22}$$

or

$$F[IX]=\frac{kf}{\lambda^3}\overline{T}_l F\left\{\int_{-\infty}^{\infty}\exp\left(-\frac{|x-s|}{\lambda}\right)H(|s|)\,\mathrm{d}s\right\} \tag{23}$$

where $H(|s|)=1$ for $-\infty<s<\infty$. Therefore:

$$F[IX] = \frac{kf}{\lambda^3}\overline{T_l}F\left\{\int_{-\infty}^{\infty}\exp\left(-\frac{|x-s|}{\lambda}\right)\right\}F\{H(|s|)\,ds\} \le \frac{kf}{\lambda^3}\overline{T_l}\frac{2\lambda}{\omega^2\lambda^2+1}\delta(\omega) \quad (24)$$

where $\delta(\omega)$ is the Dirac delta function. Since this function only has a value of 1 at $\omega = 0$, then the transform is:

$$\frac{kf}{\lambda^2}\overline{T_l} \quad (25)$$

Using these results, the Eqs. (13) and (15) can be Fourier transformed, the result of which is:

$$\overline{\frac{\partial}{\partial t}\left[\rho CpT_l + \tau_s\rho Cp\frac{\partial T_l}{\partial t}\right]} = \frac{kf}{\lambda^3}\left[\frac{2\lambda}{\omega^2\lambda^2+1}\overline{T_e}\right] - \frac{kf}{\lambda^2}\overline{T_l} + \left[\frac{I_o\delta f}{2\lambda}\right]\left[\frac{2\lambda}{\omega^2\lambda^2+1}\right]\left[\frac{2\delta}{\delta^2+\omega^2}\right] \quad (26)$$

and

$$\frac{k}{\lambda^2}[\overline{T_e} - f\overline{T_l}] = \left[\frac{k(1-f)}{\lambda^3}\right]\left[\frac{2\lambda}{\omega^2\lambda^2+1}\right]\overline{T_e} + \frac{I_o\delta(1-f)}{2\lambda}\left[\frac{2\lambda}{\omega^2\lambda^2+1}\right]\left[\frac{2\delta}{\delta^2+\omega^2}\right] \quad (27)$$

If the transform function $\overline{T_e}$ is obtained from Eq. (26) using Eq. (27), the result is:

$$\left[f\left(1+\tau_s\frac{\overline{\partial T_l}}{\partial t}\right)+\omega^2\lambda^2\right]\overline{\frac{\partial}{\partial t}(\rho CpT_l)} = -\omega^2kf\overline{T_l} + I_o\delta f\left[\frac{2\delta}{\delta^2+\omega^2}\right] \quad (28)$$

New multiplication in the transform domain by $(i\omega)^2$ corresponds to second order differential in the real plane. Hence the inversion of the above equation gives:

$$\left[f\left(1+\tau_s\frac{\partial T_l}{\partial t}\right) - \frac{\lambda^2\partial^2}{\partial x^2}\right]\rho Cp\frac{\partial T_l}{\partial t} = kf\frac{\partial^2 T_l}{\partial x^2} + I_o\delta f\exp(-\delta|x|) \quad (29)$$

If the terms $(\lambda^2/f)\partial^2/\partial x^2(\rho Cp(\partial T_l/\partial t))$ and $f\tau_s(\partial/\partial t)\times(\rho Cp(\partial T_l/\partial t))$ are neglected for all f values, equation (29) becomes:

$$\rho Cp\frac{\partial T_l}{\partial t} = k\frac{\partial^2 T_l}{\partial x^2} + I_o\delta\exp(-\delta|x|) \quad (30)$$

which is the same as a Fourier heat-conduction equation.

The Eq. (29) can be re-written as:

$$\rho Cp\frac{\partial T_l}{\partial t} = k\frac{\partial^2 T_l}{\partial x^2} + f\frac{\lambda^2\partial^2}{\partial x^2}\left(\rho Cp\frac{\partial T_l}{\partial t}\right) - \rho Cp\tau_s\frac{\partial^2 T_l}{\partial t^2} + I_o\delta\exp(-\delta|x|) \quad (31)$$

Eq. (31) is a third order partial differential equation, which can be decomposed into second and third order two differential equations, i.e., when Eq. (31) is decomposed into two equations, the resulting probable differential equations are:

$$A\frac{\partial T_e}{\partial t} = B\frac{\partial^2 T_e}{\partial x^2} - C[T_e - T_l] + I_o\delta\exp(-\delta|x|)$$
$$D\frac{\partial T_l}{\partial t} = C[T_e - T_l] \quad (32)$$

where A, B, C, and D are the coefficients. To find the values of A, B, C, and D, the following procedure is adopted, i.e.:

$$D\frac{\partial^2 T_l}{\partial t^2} = C\left[\frac{\partial T_e}{\partial t} - \frac{\partial T_l}{\partial t}\right] \quad (33)$$

or:

$$\frac{\partial T_e}{\partial t} = \frac{D}{C}\frac{\partial^2 T_l}{\partial t^2} + \frac{\partial T_l}{\partial t} \quad (34)$$

Similarly:

$$D\frac{\partial^2}{\partial x^2}\left(\frac{\partial T_l}{\partial t}\right) = C\left[\frac{\partial^2 T_e}{\partial x^2} - \frac{\partial^2 T_l}{\partial x^2}\right] \quad (35)$$

or:

$$\frac{\partial^2 T_e}{\partial x^2} = \frac{D}{C}\frac{\partial^2}{\partial x^2}\left(\frac{\partial T_l}{\partial t}\right) + \frac{\partial^2 T_l}{\partial x^2} \quad (36)$$

Substitution of Eqs. (34) and (36) into Eq. (31) yields:

$$(D+A)\frac{\partial T_l}{\partial t} = \frac{BD}{C}\frac{\partial^2}{\partial x^2}\left(\frac{\partial T_l}{\partial t}\right) + B\frac{\partial^2 T_l}{\partial x^2} - \frac{AD}{C}\frac{\partial^2 T_l}{\partial t^2} + I_o\delta\exp(-\delta|x|) \quad (37)$$

After equating Eqs. (37) and (31), the coefficients A, B, C, and D can be calculated, i.e.:

$$A = \frac{fk\tau_s}{\lambda^2}$$
$$B = k$$
$$C = \frac{fk}{\lambda^2}\left(1 - \frac{k\tau_s}{\rho Cp\lambda^2}\right)$$
$$D = \rho Cp - \frac{fk\tau_s}{\lambda^2} \quad (38)$$

Eq. (32) is identical to Eq. (1) given in the two-equation model. Consequently, setting the coefficients of Eqs. (32) and (1), it yields:

$$\frac{fk\tau_s}{\lambda^2} = Ce$$
$$\frac{fk}{\lambda^2}\left(1 - \frac{k\tau_s}{\rho Cp\lambda^2}\right) = G \tag{39}$$
$$\rho Cp - \frac{fk\tau_s}{\lambda^2} = C_l$$

where $\tau_s = G/C_e$ [21] and $C_e = \gamma T_e$ (where γ is constant and $\gamma = 67.6$ J/m^3 K^2 for gold [22]). Moreover, the electron–phonon coupling factor is temperature dependent, which can be written as [23]:

$$G = \frac{\pi^2 m_e N \overline{V}^2}{6\tau_p T_e} \tag{40}$$

Temperature dependent electron thermal conductivity can be formulated as [22]:

$$k = \frac{1}{3}\frac{\overline{V}^2 C_e}{aT_l + bT_e^2} \tag{41}$$

where a and b are constants, i.e.: $a = 1.23 \times 10^{11}$ (1/sK) and $b = 1.2 \times 10^7$ (1/sK^2).

2.3. Numerical solution

The numerical method employed uses a finite difference scheme, which is well established in the literature [24]. In order to obtain accurate results, the convergency criteria should be met. The stability criteria for the heating model is as follows:

$$1 \geq ABS\left[\frac{f\rho Cp}{\Delta t} + 2\lambda^2\rho Cp\left[\frac{1}{\Delta t(\Delta x)^2}\right] - 2kf\left[\frac{1}{(\Delta x)^2}\right]\right] + ABS\left[\frac{kf}{(\Delta x)^2} - \frac{2\lambda^2\rho Cp}{\Delta t(\Delta x)^2}\right] + ABS\left[\frac{2\lambda^2\rho Cp}{\Delta t(\Delta x)^2}\right] - ABS\left\{\frac{f\rho Cp}{\Delta t} + 2\lambda^2\rho Cp\left[\frac{1}{\Delta t(\Delta x)^2}\right]\right\} \tag{42}$$

where Δx is spatial increments in the x axis while Δt is the time increment.

In the numerical solution of Eq. (32), the coefficients A, B, C, and D are defined through f, λ, k, and τ_s, which are determined from Eqs. (38)–(41), since temperature dependent G, k and τ_s are known, from $\tau_s = G/C_e$, and Eqs. (40) and (41).

Thermophysical properties of gold at 100 K and laser pulse properties used in the computations are given in Tables 1 and 2.

3. Results and discussion

Laser shortpulse heating of gold with variable properties is considered. An electron kinetic theory approach is introduced when modelling nonequilibrium heating process. The governing integro-differential equations are reduced to differential equation, which is then deformed into two differential equations. The coefficients of the differential equations are compared with the coefficients of the equations in two-equation model. The heating period considered in the present study is in the order of 0.2–1 ps, therefore, the electron kinetic theory model based on the collisional energy transport is appropriate to describe the physical processes taking place in this time domain, i.e. the time duration considered is longer than the electron–phonon interaction duration, which is in the order of 0.02 ps at room temperature [23]. Consequently, the models developed for ultra-short-pulses (Hyperbolic-two-step model [25] and Ballistic model [13]) are not considered in the present study.

Fig. 2 shows electron temperature distribution inside the substrate material for constant and variable properties and two heating periods. Electron temperature attains high values for a constant properties case. This is more pronounced at long heating period (10^{-12} s). In this case, electron–phonon coupling constant reduces as electron temperature increases. This in turn enhances excess electron energy transfer to lattice site through a collisional process. Moreover, as the heating period progresses, energy absorbed by electrons increases, which results in increased electron excess energy. Con-

Table 1
Thermal properties of gold at 100 K

T_d (K)	γ (J/m^3 K^2)	$\delta \times 10^7$ (1/m)	$m \times 10^{-31}$ (kg)	$C_l \times 10^6$ (J/Km^3)	k (W/m K)	$G \times 10^{16}$ (W/m^3 K)	τ_s (ps)	$N \times 10^{28}$ (1/m^{-3})	$\overline{V}$ (m/s)
343	67.6	7.1	9.1	2.8	315	3.5	0.276	8.4	5010

Table 2
The coefficients and the range of values used in the simulations

λ (m)	f	$A \times 10^4$ (W/m^3 K)	B (W/m K)	$C \times 10^{16}$ (W/m^3 K)	$D \times 10^6$ (J/m^3 K)	$I_o(1 - r_f)$ (W/m^2)
10^{-9}–10^{-10}	10^{-1}–10^{-5}	2.52–2.09	315	3.12–2.59	2.47–2.49	1×10^{13}

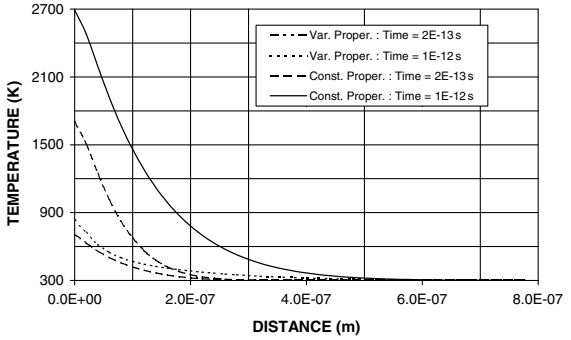

Fig. 2. Electron temperature distribution inside the substrate material for constant and variable properties and two time periods.

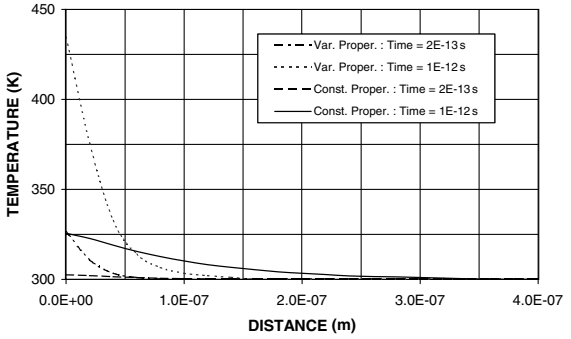

Fig. 3. Lattice site temperature distribution inside the substrate material for constant and variable properties and two time periods.

sequently, for the constant properties case, where electron–phonon coupling factor is low, less electron excess energy transfers to the lattice site. The magnitude of electron temperature, therefore, increases considerably for a constant properties case. The temperature gradient corresponding to a constant properties case attains higher values than that corresponding to a variable properties case. This is because of the electron–phonon coupling factor, which attains high values at high electron temperatures as seen from Fig. 7. The low levels of electron–phonon coupling factor results in less electron excess energy transferring to lattice site; consequently, electron energy remains high in the surface vicinity. Moreover, the absorption in the substrate material is governed by the Lambert's law, in which case, absorbed energy decays exponentially with increasing depth in the substrate material. The energy absorbed by electrons reduces as the distance from the surface increases towards the solid bulk. Therefore, less energy transporting to lattice site and reducing amount of absorbed energy with increasing depth results in sharp decay of electron temperature at some depth below the surface. In the case of a variable properties, high magnitude of electron–phonon coupling increases the rate of electron excess energy transferring to lattice site despite the low electron excess energy at some depth below the surface due to absorption of irradiated energy, which reduces exponentially. Moreover, the rate of excess energy gain of electrons is high in the surface vicinity of the substrate material, which in turn results in high electron temperature and relatively lower temperature gradient in this region ($x < 3 \times 10^{-8}$ m), i.e. electrons with high energy can transfer more amount of their excess energy to lattice site in this region as compared to some depth next to the surface vicinity. This is more pronounced for a constant properties case.

Fig. 3 shows lattice site temperature distribution inside the substrate material for constant and variable properties and two heating periods. Temperature attains high values in the surface vicinity for a variable properties case. In this case, high rate of electron excess energy transferring to lattice site, due to high electron–phonon coupling factor, results in high levels of lattice site energy gain in this region. In the case of constant properties, lattice site temperature attains lower values than that corresponding to a variable properties case. This is more pronounced at long heating periods. The temperature gradient corresponding to a variable properties case is higher than that corresponding to a constant properties case. This occurs because of the excess electron energy transfer mechanism. When comparing electron and lattice site temperature distributions, it can be observed that both temperature profiles do not behave similar, i.e. the lattice site temperature gradient is higher than the electron temperature gradient. This indicates that electrons do not transfer their excess energy as they gain from the irradiation field. In this case, electrons gain more energy through the absorption and transfer less energy to lattice site through collisional process.

Fig. 4 shows temporal variation of electron temperature for constant and variable properties and two

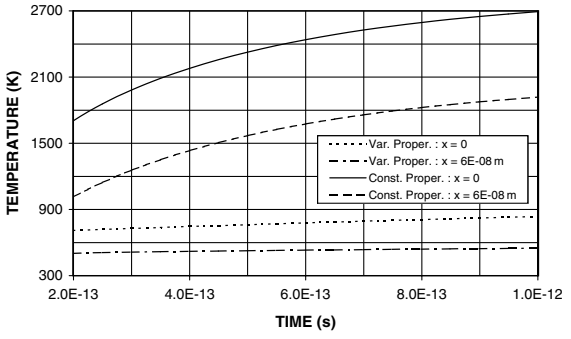

Fig. 4. Temporal variation of electron temperature distribution for constant and variable properties and two locations inside the substrate material.

locations inside the substrate material. Electron temperature rises rapidly in the early heating period and the rate of temperature rise reduces as the heating period progresses. This is because of the excess energy gain of electrons from the irradiated field. In this case, electrons gain substantial energy from the irradiated field and transfer considerably less energy to lattice site due to few number of collisions taking place in the early heating period. As the heating period progresses, some high fraction of electron excess energy transfers to lattice site due to large number of collisions taking place during the long duration of heating period. This suppresses the rapid rise of electron temperature. Moreover, electron temperature attains almost steady at some depth below the surface. This occurs because of electrons absorbing less energy from the irradiated field, since amount of energy absorbed reduces with increasing depth (Lambert's law). In addition, electrons moving from the surface to the solid bulk loss some of their excess energy through collisional process. Consequently, electron excess energy reduces as the depth below the surface increases.

Fig. 5 shows temporal variation of lattice site temperature for constant and variable properties cases and two different locations inside the substrate material. The rate of lattice site temperature rise is considerably small in the early heating period ($t = 2 \times 10^{-13}$ s). This is because of few number of collisions taking place in this period. As the heating period progresses, the rate of temperature rise becomes steady, which is true for all cases shown in the figure. The steady temperature rise indicates that the rate of electron excess energy transfer to lattice site becomes steady with progressing time. Moreover, the rate of temperature rise for a variable properties case is higher than that corresponding to a constant properties case. This is due to electron–phonon coupling factor, which attains high values for variable properties case as seen from Fig. 7. The electron–phonon coupling factor decays gradually with progressing time although the rate of energy transferring to lattice site remains almost steady. This is because of the

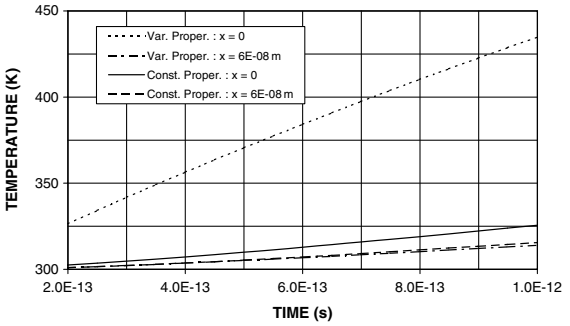

Fig. 5. Temporal variation of lattice site temperature distribution for constant and variable properties and two locations inside the substrate material.

fact that electron excess energy increases with progressing time due to absorption process, which in turn increases the amount of electron excess energy transferring to lattice site. However, gradual reduction in electron–phonon coupling factor suppresses the amount of energy transfer to lattice site. Consequently, enhancement of electron excess energy and suppression of electron–phonon coupling factor with increasing heating period result in almost steady rise in lattice site temperature.

Fig. 6 shows temperature dependent electron specific heat capacity while Fig. 7 shows electron–phonon coupling factor, respectively. Specific heat capacity decays with increasing distance from the surface as similar to electron temperature, since $C_e = \gamma T_e$ where $\gamma = 67.6$ J/m^3 K^2. Consequently, temporal and spatial behavior of specific heat capacity is similar to the behavior of electron temperature. In the case of electron–phonon coupling, it decays sharply in the surface region of the substrate material. The decay rate does not follow electron temperature, since it depends on the mean velocity ($\overline{V}$), characteristic time (τ_s), and electron and lattice site temperatures (T_e and T_l). In the early heating period electron–phonon coupling factor increases rapidly similar to electron temperature rise. This indicates that increasing electron temperature improves the

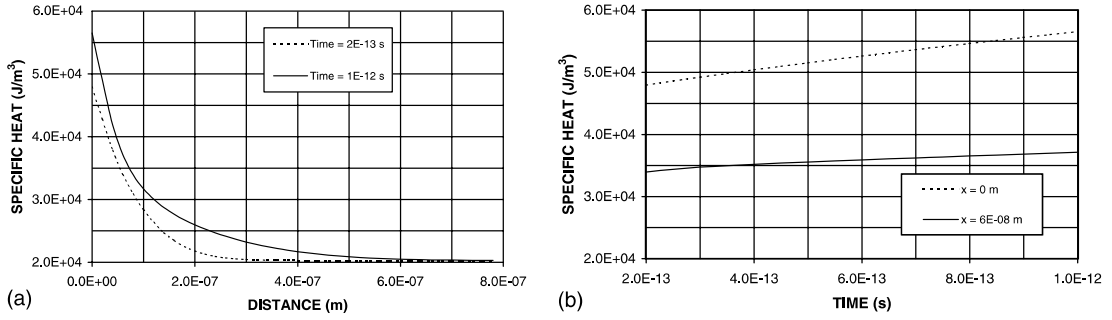

Fig. 6. (a) Specific heat capacity distribution inside the substrate material for two heating periods. (b) Temporal variation of specific heat capacity for two locations inside the substrate material.

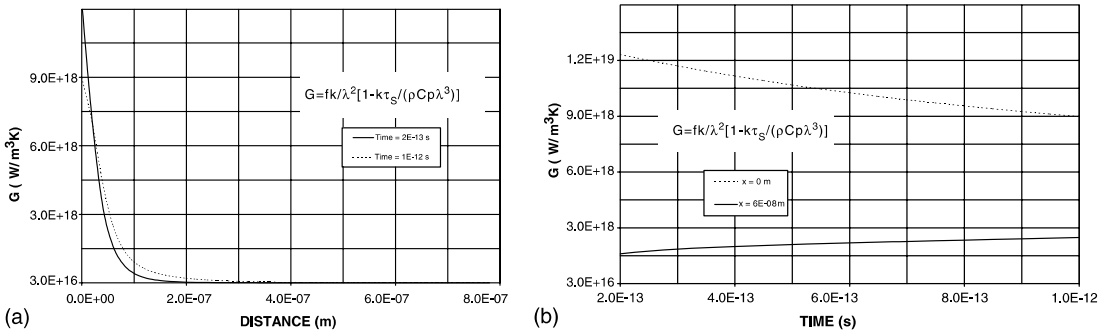

Fig. 7. (a) Electron–phonon coupling constant distribution inside the substrate material for two heating periods. (b) Temporal variation of electron–phonon coupling constant for two locations inside the substrate material.

energy transfer mechanism, i.e. in general, electron–phonon coupling factor increases.

4. Conclusions

Laser shortpulse heating is considered and gold with variable and constant properties are employed in the simulations. Electron kinetic theory approach is introduced when modelling the nonequilibrium energy transport process. The integro-differential equations are reduced to partial differential equations. The coefficients of partial differential equations are related with the coefficients of those equations given in two-equation model. It is found that variable properties has a significant effect on electron and lattice site temperature rises in the substrate material. In this case, a constant properties case results in low electron and high lattice site temperatures. The electron–phonon coupling factor rises rapidly in the early heating period as electron temperatures increases in this domain. Moreover, as the heating progresses electron temperature rises steadily while electron–phonon coupling reduces gradually. This results in steady rise of lattice site temperature with progressing heating period. Electron and lattice site temperatures rise at a slow rate at some depth below the surface, which is because of the energy absorbed by electrons from the irradiated field, which decays according to the Lambert's law. The rapid rise of electron temperature in the early heating period is due to electron excess energy transfer process; in which case, electrons transfer less energy to lattice site through few number of collisions in the early heating period.

Acknowledgements

The author acknowledge the support of King Fahd University of Petroleum and Minerals, Dhahran, Saudi Arabia, for this work.

Appendix A. Formulation of f

The fraction of electron excess energy transfer during the time comparable or greater than the electron–phonon characteristic time (τ_s) can be written in terms of the energy balance across the section dx in the substrate material, i.e.:

$$f = \frac{(\text{Electron energy})_{\text{in}} - (\text{Electron energy})_{\text{out}}}{(\text{Electron energy})_{\text{in}} - (\text{Phonon Energy})}$$

or

$$f = \frac{(T_{\text{e}})_{\text{in}} - (T_{\text{e}})_{\text{out}}}{(T_{\text{e}})_{\text{in}} - T_{\text{l}}} \tag{43}$$

where $(T_{\text{e}})_{\text{in}}$ is the temperature of an electron entering the section, $(T_{\text{e}})_{\text{out}}$ temperature of the an electron leaving the section, and T_{l} is the phonon temperature. f takes the values $0 \leq f \leq 1$.

References

[1] S.I. Anisimov, A.M. Bonch-Bruevich, M.A. El'yashevich, Y.A. Imas, N.A. Pavlenko, G.S. Romanov, Effect of powerful light fluxes on metals, Sov. Phys.-Tech. Phys. 11 (1967) 945–952.
[2] J.F. Luciani, P. Mora, J. Virmont, Nonlocal heat transport due to steep temperature gradients, Phys. Rev. Lett. 51 (1983) 1664–1667.
[3] J.G. Fujimoto, J.M. Liu, E.P. Ippen, Femtosecond laser interaction with metallic tungsten and nonequilibrium electron and lattice temperatures, Phys. Rev. Lett. 53 (1984) 1837–1840.
[4] H.E. Elsayed-Ali, T.B. Norris, M.A. Pessot, G.A. Mourou, Time-resolved observation of electron–phonon relaxation in copper, Phys. Rev. Lett. 58 (12) (1987) 1210–1215.
[5] S.D. Brorson, A. Kazeroonian, J.S. Moodera, D.W. Face, T.K. Cheng, E.P. Ippen, M.S. Dresselhaus, G. Dresselhaus, Femtosecond room-temperature measurement of the electron–phonon coupling constant λ in metallic superconductors, Phys. Rev. Lett. 64 (1990) 2172–2175.
[6] P.B. Allen, Theory of thermal relaxation of electrons in metals, Phys. Rev. Lett. 59 (1987) 1460–1463.

[7] L.G. Hector Jr., W.S. Kim, M.N. Ozisik, Hyperbolic heat conduction due to mode locked laser pulse train, Int. J. Engng. Sci. 30 (1992) 1731–1744.
[8] A. Kar, C.L. Chan, J. Mazumder, Comparative studies on nonlinear hyperbolic heat conduction for various boundary conditions: analytical and numerical solutions, ASME, J. Heat Transfer 114 (1992) 14–20.
[9] L. Malinowski, A relaxation model for heat conduction and generation, J. Phys. D: Appl. Phys. 26 (1993) 1176–1180.
[10] H. Strehlow, Heating of opaque surfaces by picosecond laser pulses, Appl. Phys. A 45 (1997) 355–360.
[11] T.Q. Qiu, C.L. Tien, Size effects on nonequilibrium laser heating of metals, ASME, J. Heat Transfer 115 (1993) 842–847.
[12] D.Y. Tzou, A unified field approach for heat conduction from macro-to-micro-scales, ASME, J. Heat Transfer 117 (1995) 8–16.
[13] G. Cheng, Ballistic-diffusive heat-conduction equations, Phys. Rev. Lett. 86 (2001) 2297–2300.
[14] B.S. Yilbas, Heating of metals at a free surface by laser radiation an electron kinetic theory approach, Int. J. Engng. Sci. 24 (8) (1986) 1325–1334.
[15] B.S. Yilbas, S.Z. Shuja, Laser short-pulse heating of surfaces, J. Phys. D: Appl. Phys. 32 (1999) 1947–1954.
[16] B.S. Yilbas, Laser short-pulse heating: moving heat source and convective boundary considerations, Physica A 203 (2001) 157–177.
[17] G.L. Eesley, Generation of nonequilibrium electron and lattice temperatures in copper by picosecond laser pulses, Phys. Rev. B 33 (1986) 2144–2151.
[18] B.S. Yilbas, M. Sami, 3-Dimensional laser heating including evaporation—a kinetic theory approach, Int. J. Heat Mass Transfer 41/13 (1998) 1969–1981.
[19] B.S. Yilbas, Electron kinetic theory approach—one-and three-dimensional heating with pulsed laser, Int. Heat Mass Transfer 44 (2001) 1925–1936.
[20] C.L. Tien, J.H. Lienhard, Statistical Thermodynamics, Hemisphere, Washington DC, 1979.
[21] B.S. Yilbas, A.Z. Sahin, An approach to convergency of kinetic theory to Fourier theory in relation to laser heating process, Jpn. J. Appl. Phys. 32 (Part 1 12A) (1993) 5646–5651.
[22] X.Y. Wang, D.M. Riffe, Y.S. Lee, M.C. Downer, Time-resolved electron-temperature measurement in a highly excited gold target using femtosecond thermionic emission, Phys. Rev. B 50 (1994) 8016–8019.
[23] T.Q. Qiu, C.L. Tien, Short-pulse laser heating on metals, Int. J. Heat Mass Transfer 35 (1992) 719–726.
[24] G.D. Smith, Numerical Solution of Partial Differential Equations: Finite Difference Methods, third ed., Clarendon Press, Oxford, 1985.
[25] T.Q. Qiu, C.L. Tien, Femtosecond laser heating of multi-layer metals-I. analysis, Int. J. Heat Mass Transfer 37 (1992) 2789–2797.